

A High Intrinsic Peculiarity Rate Among Type Ia Supernovae

Weidong Li, Alexei V. Filippenko, Richard R. Treffers
Department of Astronomy, University of California, Berkeley, CA 94720-3411

Adam G. Riess
Space Telescope Science Institute, 3700 San Martin Drive, Baltimore, MD 21218
and

Jingyao Hu and Yulei Qiu
Beijing Astronomical Observatory, Chinese Academy of Sciences, Beijing 100080, P. R. C.

Received _____; accepted _____

ABSTRACT

We have compiled a sample of 45 Type Ia supernovae (SNe Ia) discovered by the Lick Observatory Supernova Search (LOSS) and the Beijing Astronomical Observatory Supernova Survey (BAOSS), and determined the rate of spectroscopically peculiar SNe Ia (i.e., SN 1986G-like, SN 1991bg-like, and SN 1991T-like objects) and the luminosity function of SNe Ia. Because of the nature of the two surveys (distance-limited with small baselines and deep limiting magnitudes), nearly all SNe Ia have been discovered in the sample galaxies of LOSS and BAOSS; thus, the observed peculiarity rate and luminosity function of SNe Ia are intrinsic. We find that $36\pm 9\%$ of nearby SNe Ia are peculiar; specifically, the luminosity function of SNe Ia consists of 20% SN 1991T-like, 64% normal, and 16% SN 1991bg-like objects. We have compared our results to those found by earlier studies, and to those found at high redshift. The apparent dearth of SN 1991T-like objects at high redshift may be due to extinction, and especially to the difficulty of recognizing them from spectra obtained past maximum brightness or from spectra with low signal-to-noise ratios. Implications of the high peculiarity rate for the progenitor systems of SNe Ia are also briefly discussed.

Subject headings: methods: statistical – supernovae: general – supernovae: progenitors

1. Introduction

Supernovae (SNe) are classified as Type Ia on the basis of distinguishing features in their optical spectra (e.g., Harkness & Wheeler 1990). During the early photospheric phase, for example, SN Ia spectra lack conspicuous lines of hydrogen and contain a strong absorption feature at about 6150 Å due to blueshifted Si II λ 6355. The inferred expansion velocity of the ejecta is more than 10,000 km s⁻¹, implying a violent explosion.

A striking characteristic of SNe Ia is that they display a remarkable degree of similarity, more than any other subclass of SNe, and their spectral evolution follows a reproducible pattern (e.g., Kirshner et al. 1973; Branch & Tammann 1992; Wells et al. 1994; Filippenko 1997). The light curves of SNe Ia are also impressively homogeneous (e.g., Leibundgut et al. 1992; Branch & Tammann 1992). At maximum brightness the color is strongly peaked near $B - V = 0$ mag (Patat et al. 1997), and the absolute magnitude has a much smaller dispersion than in other subclasses of SNe. For example, the dispersion of the Calán/Tololo Survey is only ~ 0.2 mag when a few observationally red SNe Ia are excluded (Hamuy et al. 1996). Thus, SNe Ia have been considered homogeneous and used as “standard candles” (see Branch & Tammann 1992 for a review).

As summarized by Filippenko (1997) and in Section 2, however, the existence of the peculiar SN Ia 1986G and the appearance of two very peculiar SNe Ia (1991T and 1991bg) in the same year have drawn attention to diversity among SNe Ia. These variations have raised concerns about the cosmological utility of SNe Ia. In an attempt to quantify the rate of spectroscopically peculiar SNe Ia in the existing observed sample, Branch, Fisher, & Nugent (1993, hereafter BFN) compiled a set of 84 SNe Ia, and subclassified them as either normal or like one of the known peculiar SNe Ia: SN 1986G, SN 1991T, or SN 1991bg. They found that their sample is affected by the Malmquist bias; nevertheless, about 83% to 89% of their sample is normal. Even among the relatively normal SNe Ia, however, there are observed differences in spectra and light curves (e.g., Filippenko 1997; Hamuy et al. 1996; Riess et al. 1999a). Fortunately, the variation in luminosity is correlated with light-curve shape, providing a means to calibrate the peak luminosity of SNe Ia [e.g., the $\Delta m_{15}(B)$ method – Phillips 1993, Hamuy et al. 1996, Phillips et al. 1999; the multi-color light-curve shape method – Riess, Press, & Kirshner 1996, Riess et al. 1998; the stretch method – Perlmutter et al. 1997]. Moreover, the photometric sequence exhibited by SNe Ia represents a spectroscopic sequence, from overluminous (by ~ 0.4 mag in V) SN 1991T-like objects to subluminous (by ~ 2 mag in V) SN 1991bg-like objects (Nugent et al. 1995).

The intrinsic peculiarity rate of SNe Ia has implications for our understanding of SNe Ia, especially their progenitor systems. SNe Ia are thought to come from thermonuclear explosions of mass-accreting white dwarfs in binary systems, when their masses reach the critical Chandrasekhar mass ($\sim 1.4 M_{\odot}$; for a review see Branch et al. 1995). The exact nature of the progenitors, however, is still controversial, and many scenarios have been proposed. If the majority of SNe Ia are normal, we might expect SNe Ia to come from one

class of progenitor system, and the peculiar SNe Ia to come from some variation of the same system; on the other hand, if a significant fraction of SNe Ia are peculiar, additional classes of progenitor systems might be warranted.

In the past several years, many SNe Ia have been discovered in the course of two successful nearby SN surveys – the Lick Observatory Supernova Search (LOSS; Treffers et al. 1997; Li et al. 2000a; Filippenko et al. 2000) with the Katzman Automatic Imaging Telescope (KAIT), and the Beijing Astronomical Observatory Supernova Survey (BAOSS; Li et al. 1996) with a 0.6-m telescope. Here we study the peculiarity rate of SNe Ia from these two surveys. In Sec. 2 we discuss the sample of SNe Ia used in the statistics, which consists of 45 SNe Ia discovered by LOSS and BOASS (up through SN 2000A). Sec. 3 reports the observed and intrinsic peculiarity rate and luminosity function. The implications of our statistics are discussed in Sec. 4, and Sec. 5 summarizes our conclusions.

2. The Sample of Type Ia SNe

2.1. Definition of Peculiar SNe Ia

As we attempt to compare our results to those of BFN, we follow their definition of normal and peculiar SNe Ia. A summary of this definition is given here; see also Filippenko (1997).

A “normal” SN Ia is defined as one whose optical spectra resemble those of SNe 1981B (Branch et al. 1983), 1989B (Barbon et al. 1990), 1992A (Kirshner et al. 1993), and 1972E (Kirshner et al. 1973). Normal SNe Ia near maximum light show conspicuous absorption features near 6150 Å due to Si II and near 3750 Å due to Ca II. Other absorption features include those of Co II, S II, O I, and Mg II, as well as additional lines of Si II and Ca II. Two weeks after maximum the Si II 6150 Å and the Ca II 3750, 8300 Å lines are strong, several Fe II lines develop at the blue end of the spectrum, and the absorption near 5700 Å is usually attributed to Na I. Blends of forbidden emission lines of iron and cobalt dominate the nebular phase, starting about a month past maximum brightness.

A “spectroscopically peculiar” SN Ia is defined as one that has feature strengths (not just expansion velocities) that differ significantly from those of the normal ones at a given phase. Three well-observed examples, SNe 1991T, 1991bg, and 1986G, serve as prototypes of peculiar SNe Ia.

Spectra of SN 1991T (Filippenko et al. 1992a; Phillips et al. 1992; Ruiz-Lapuente et al. 1992; Jeffery et al. 1992; Mazzali et al. 1995) before maximum brightness are strikingly peculiar in having unusually weak lines of Si II, S II, and Ca II, yet prominent high-excitation features of Fe III. The usual Si II, S II, and Ca II lines develop in the post-maximum spectra, and by a few weeks past maximum the spectra look nearly normal.

However, as Filippenko et al. (1992a) and Li et al. (1999) pointed out, at late times subtle differences still exist between high-quality spectra of SN 1991T-like objects and those of normal SNe Ia. SN 1999aa (Filippenko, Li, & Leonard 1999) is similar to SN 1991T (Figure 1) in having very weak Si II 6150 Å absorption and prominent Fe III lines near 4300 Å and 5000 Å, but it also shows strong absorption centered at 3750 Å that is probably due to Ca II H&K, which is very weak in SN 1991T. Whether objects like SN 1999aa (to be discussed in more detail by Li et al. 2000c) are of an intermediate type between SN 1991T-like events and normal SNe Ia remains to be determined. Not to complicate the classification scheme, however, here we still classify SN 1999aa-like objects as “SN 1991T-like,” even though most SN 1991T-like objects seem to actually be like SN 1999aa. At this time there is widespread familiarity with SN 1991T subclass, whereas SN 1999aa-like objects were only recently recognized and are unknown to most researchers. See Section 4.1 for further discussion of this issue.

The main spectral peculiarities of SN 1991bg (Filippenko et al. 1992b; Leibundgut et al. 1993; Turatto et al. 1996; Mazzali et al. 1997), when at maximum brightness, are the presence of a broad absorption trough extending from about 4100 to 4400 Å due to Ti II lines, and enhanced Si II 5800 Å absorption relative to Si II 6150 Å.

SN 1986G (Phillips et al. 1987; Cristiani et al. 1992) is similar to SN 1991bg but less extreme. The Ti II 4100-4400 Å absorption trough is present in the spectra of SN 1986G, yet is weaker than that of SN 1991bg. Since it is difficult to differentiate SN 1986G-like objects from SN 1991bg-like ones without having excellent data, we have combined the two classes together, and call them SN 1991bg-like objects hereafter, unless otherwise noted.

Various authors have shown that the spectroscopic behavior of SNe Ia is correlated with their photometric behavior, which in turn is related to their absolute magnitudes (e.g., Nugent et al. 1995; Filippenko 1997, and references therein). SN 1991T-like objects rise to their maximum more slowly and decline more slowly, and are overluminous relative to normal SNe Ia; SN 1991bg-like objects rise to their maximum and decline more quickly, and are subluminous relative to normal SNe Ia. Thus light curves, if available, can often serve as an independent check of the peculiarities of SNe Ia, though exceptions do exist (e.g., SN 1992bc, Maza et al. 1994; SN 1999ee, Hamuy 2000, private communication).

2.2. The Sample of SNe Ia

We have compiled a set of 45 nearby SNe Ia discovered in the sample galaxies of LOSS and BAOSS. This includes 38 SNe Ia discovered by LOSS and BAOSS, and 7 SNe Ia that were initially discovered by other groups, but were subsequently rediscovered in the course of LOSS or BAOSS. Table 1 lists the information for all these SNe in the following format: Column (1): SN name. Column (2): host galaxy of the SN. Column (3): the Hubble type of the host galaxy. A classification followed by a “:” means it is uncertain. Column (4):

the number of the International Astronomical Union (IAU) Circular that contains the spectroscopic classification of the SN. Column (5): the age of the SN at the time of the spectroscopic classification, relative to the time of B -band maximum brightness. This is generally *not* the age of the SN at discovery, as it takes several days (sometimes longer) for the spectroscopic classification of a SN to be made. The quoted ages are derived either from the IAU Circular listed in Column (4), which are marked with a colon and generally have uncertainties of about ± 5 days, or from our own light-curve database and/or spectral analysis, which usually have uncertainties of about ± 2 days. Column (6): discoverer of the SN. “L” means LOSS, “B” means BAOSS, and “O” means other groups. Column (7): whether the SN is peculiar. If it is, the type of peculiarity is listed. Objects marked as peculiar type “91T_{aa}” are those that are similar to SN 1999aa as discussed earlier. For SNe 1997cw and 1999gp, no spectroscopic information are available to us to determine whether they are SN 1999aa-like, and they are classified as “91T/91T_{aa}”. Columns (8) to (11): evidence of the peculiarity of the SN. Specifically, Ti II absorption (Col. 8), a relatively strong Si II 5800 Å absorption (Col. 9), prominent Fe III absorption lines (Col. 10), and weak or no Si II 6150 Å absorption (Col. 11). Our major source of information for the host galaxies of the SNe is NED¹, and that for the SNe is the IAU Circulars.

One danger of using the information in the IAUCs to subclassify a SN Ia is that it was most likely derived by the observer during, or shortly after the observations. This “on-the-fly” classification might result in quick-look reduction errors and approximations. The subclassification also depends on the observer’s ability to recognize the peculiarities in the spectra of SNe Ia and the willingness to include the information in the report to the IAUC. Sometimes classifications of SNe in the IAUCs are revised because of subsequent observations or reductions. For this reason, we count a SN Ia as peculiar only when there is direct evidence of peculiarity included in the classification of the SN in IAUCs, or we have our own spectra to support the classification. Columns (8) to (11) in Table 1 list the evidence reported in the relevant IAUCs. A SN is classified as SN 1999bg/1986G-like only when there is evidence in the IAUC that its spectrum shows Ti II absorption and a relatively strong Si II 5800 Å line, while a SN 1991T-like object must show evidence of Fe III absorption lines and weak (or absent) Si II lines.

We have classified two SNe as peculiar even though they were not listed as such in the IAUCs. SN 1999bh was discovered by LOSS (Li 1999). Aldering et al. (1999) reported that the spectrum was of a SN Ia within one week after maximum brightness. Nugent (1999) communicated that Aldering’s spectrum of SN 1999bh resembled SN 1986G at 3 days past maximum. In addition, comparisons of its spectrum at a month past maximum to that of a normal SN Ia (SN 1998bu; Jha et al. 1999) and a SN 1991bg-like SN Ia (SN 1997cn;

¹The NASA/IPAC Extragalactic Database (NED) is operated by the Jet Propulsion Laboratory, California Institute of Technology, under contract with the National Aeronautics and Space Administration.

Turatto et al. 1998) at comparable epochs (Figure 2) reveal that SN 1999bh is similar to SN 1997cn at this phase. We thus classify SN 1999bh as a SN 1986G/1991bg-like object.

SN 1999dg was also discovered by LOSS (Modjaz & Li 1999). Filippenko, Metzger, & Small (1999) classified it as a SN Ia within a week past maximum brightness. A spectrum of the SN is shown in Figure 1. Apparent Ti II absorption is seen at around 4100-4300 Å, and the Si II absorption at 5800 Å is relatively strong. We classify SN 1999dg as a SN 1986G/1991bg-like object.

3. Statistics

3.1. The Observed Peculiarity Rate

Out of the 45 SNe in our sample, 9 are SN 1991T-like and 7 are SN 1991bg-like. The total peculiarity rate is $36\pm 9\%$. The rate for SN 1991T-like objects is $20\pm 7\%$, and for SN 1991bg-like objects it is $16\pm 6\%$. The uncertainties quoted here are derived only from Poisson statistics. Our total peculiarity rate is substantially higher than the BFN result (less than 17%); details are presented in Sec. 4.2.

3.2. The Intrinsic Peculiarity Rate

Because of the variations among the luminosities, light-curve shapes, and spectral evolution of different kinds of SNe Ia, there are several possible observational biases in the observed SN sample, and the observed peculiarity rate could be either an overestimate or an underestimate of the intrinsic peculiarity rate. The relationship between the observed and the intrinsic peculiarity rates largely depends on the way the SNe are discovered – that is, on the survey methods.

SN surveys can be generally divided into two categories, magnitude-limited and distance-limited. In a magnitude-limited SN survey, the target fields are usually random regions on the sky that contain many galaxies at different redshifts. The number of SNe discovered depends on the detection limit of the images (hence magnitude-limited). Target fields for a distance-limited SN survey, on the other hand, are individual galaxies or clusters of galaxies. The limiting magnitude of the survey images may be much deeper than all the possible SNe in the sample galaxies or clusters (as long as they aren't heavily extinguished), so the number of SNe discovered largely depends on the number and distances of the sample galaxies or clusters (hence distance-limited). A few SN surveys can be best described as a hybrid of these two categories. They are distance-limited, but many of the discovered SNe are in the background of the target galaxies and some of them have magnitudes close to the detection limit of the survey images.

Li et al. (2000b; hereafter Paper I) have used Monte Carlo simulations to study various observational biases of SN Ia observations in SN surveys. They found that there are four main observational biases. The “age bias,” which is caused by the fact that SN 1991T-like objects can only be easily identified with spectra taken prior to or near maximum brightness; the Malmquist bias, which is caused by the difference in luminosity among SNe Ia; the “light-curve shape bias,” which is caused by the difference in the light-curve shapes of SNe Ia; and the “extinction bias,” which is caused by the fact that SN 1991T-like objects often occur in dusty, star-forming regions and may suffer more extinction than the other objects. They also found that the effect of these biases depends on the characteristics of the SN survey, such as distance-limited or magnitude-limited, baseline, and limiting magnitude. The adopted cutoff for the age bias and the assumed extra extinction applied to SN 1991T-like objects for the extinction bias also play important roles in determining the results of the observations. One result from the simulations (Figures 11 and 15 in Paper I) is that for a distance-limited survey conducted in the R band with (a) the limiting distance set to where normal SNe Ia have a peak apparent magnitude of 16.0, (b) a limiting magnitude of 19.0, and (c) a baseline of ≤ 10 days, all the observational biases play negligible roles (even for extreme cases such as a cutoff of 1 day before maximum light for the age bias, and an extra extinction of 0.8 mag for SN 1991T-like objects) and all SNe Ia are found in the survey, yielding the intrinsic peculiarity rate and the luminosity function of SNe Ia.

LOSS searches about 5000 fields containing 6000 galaxies, most of which have radial velocities less than $8,000 \text{ km s}^{-1}$. BAOSS searches about 3000 fields containing some 4,000 target galaxies (BAOSS has a larger field of view than LOSS), most of which have radial velocities less than $6,000 \text{ km s}^{-1}$. For the period of this study, most galaxies in the two searches overlapped, but whereas BAOSS searches more galaxies in the winter season when it has good weather, LOSS searches more galaxies in the summer season for the same reason. Both surveys are conducted in unfiltered mode, whose closest match to the standard passbands is R . Using a Hubble constant of $65 \text{ km s}^{-1} \text{ Mpc}^{-1}$, and an absolute magnitude of normal SNe Ia of $M(B) = -19.5$, we derive that the limiting distances for LOSS and BAOSS are where normal SNe Ia have apparent peak magnitudes of 16.0 and 15.3, respectively. Figure 3 shows the number of galaxies in the LOSS sample versus the expected peak apparent magnitude of normal SNe Ia. We see that more than 96% of the expected SNe Ia in the sample galaxies have peak apparent magnitudes brighter than 16 (the dashed vertical line). The usual survey images of LOSS and BAOSS have a limiting magnitude of about 19.0, much fainter than the faintest normal, unextinguished SNe Ia in the samples. The two surveys are thus limited by the distances of their sample galaxies and belong to the distance-limited SN surveys.

Because of the high observation efficiencies (80 images per hour for LOSS and 60 for BAOSS), the two surveys have short baselines. Depending on the right ascension of the galaxies, LOSS has baselines of about 4 to 8 days and BAOSS has baselines of 4 to 10 days. Sometimes, because of spells of poor weather, the intervals between observations are longer

than 10 days for either LOSS or BAOSS, but fortunately the weather in the two surveys is largely complementary as noted above. Since most sample galaxies are in both surveys, the combined result is a baseline $\lesssim 10$ days.

The Monte Carlo simulations in Paper I indicate that for the characteristics of LOSS and BAOSS, essentially *all* SNe Ia in the LOSS and BAOSS sample galaxies should have been discovered (Figure 9 in Paper I), and the observed rates for the peculiar SNe Ia should equal their intrinsic values (Figures 11 and 15 in Paper I). [The only rare exceptions are SNe that occurred in the host galaxy nuclei that are very bright and star-like, as in the case of Seyfert galaxies, and SNe that occurred in galaxies that are well past the meridian at the beginning of the night, which the two surveys don't monitor much (Filippenko et al. 2000; Li et al. 2000a).] This means that (1) the observed peculiarity rate (36%) in our sample is close to the intrinsic one, and the 1σ uncertainty of the rate is $\pm 9\%$ according to Poisson statistics; and (2) the observed luminosity function of SNe Ia is intrinsic: SN 1991bg-like objects are $16\pm 6\%$, normal objects are $64\pm 12\%$, and SN 1991T-like objects are $20\pm 7\%$ of the total SN Ia sample.

4. Discussion

4.1. Caveats Concerning the High Peculiarity Rate

In discussing the high peculiarity rate of SNe Ia found by LOSS and BAOSS, it is relevant to ask whether this galaxy sample is representative of the general population of galaxies. For example, the sample would be biased if the galaxies were selected to be predominantly spirals rather than ellipticals, since the former have a higher SN rate than the latter. It is not entirely clear how such a selection bias would affect the resulting peculiarity rate and luminosity function of SNe Ia, because the relation between the distribution of peculiar SNe Ia and Hubble types of the host galaxies is still uncertain. This bias, however, is only present in the BAOSS sample during its first year of operation (1996, not included in the current study), when there were few elliptical galaxies in the sample. The situation was corrected at the beginning of 1997, when a totally new sample was constructed without any selection bias against particular Hubble types of galaxies (except, perhaps, the Ir and dwarf galaxies, which are under-represented in all galaxy catalogs). A comparison of the Hubble-type distribution of the galaxies in the LOSS sample, which is constructed in the same way as the BAOSS sample but extends to larger redshifts, with that of about 9,800 galaxies having $cz \leq 8,000$ km s⁻¹ in the catalog of de Vaucouleurs et al. (1991), is displayed in Figure 4. In the LOSS sample there seems to be relatively more galaxies of Hubble type Sc than other types, but the galaxies that are somewhat under-represented are actually the very late-type spirals Scd, Sd, and Sdm. The relative fraction of elliptical galaxies in the LOSS sample is about 90% of that in the de Vaucouleurs et al. (1991) catalog, so discrimination against them is not significant.

Another concern is whether the high apparent peculiarity rate of SNe Ia in the LOSS and BAOSS sample is partly caused by the fact that most of the SNe were discovered before maximum brightness, and more than half of them were discovered at least a week before maximum. At those early times, the spectrum of a SN Ia reveals the physical conditions of the outermost parts of the ejecta, where differences among individual SNe (e.g., metallicity) are most likely to reside. The high peculiarity rate found in our sample may thus be partly caused by the inhomogeneity of normal SNe Ia at early times. In particular, we are concerned with the SN 1999aa-like objects. Although we classified them as SN 1991T-like objects in the calculations of the peculiarity rates because their spectra show prominent high-excitation Fe III lines as does SN 1991T, we note the existence of prominent Ca II H&K lines in their spectra, which are weak in SN 1991T. Whether these objects are SN 1991T-like ones, or intermediate ones between SN 1991T-like and normal, or normal ones caught at very early times, remains to be determined. One way to investigate this is by studying their photometric and spectroscopic behavior (Li et al. 2000c).

To make our point more clearly, Figure 5 shows the near-maximum spectra of three SN 1999aa-like objects (SNe 1999aa, 1998es, 1999ac, all at age 1 day before maximum) and one normal object (SN 1994D at age 3 days before maximum). The overall similarity among the spectra is striking. *Had the three SN 1999aa-like objects been initially observed at this phase or later, they would have been classified as normal SNe Ia.* Unfortunately, there are no published spectra for genuine SN 1991T-like objects at this phase (e.g., SN 1991T – Filippenko et al. 1992a, Phillips et al. 1992; SN 1997br – Li et al. 1999), so it is not clear whether they showed the same spectral evolution. This comparison raises two possibilities:

(1) The SN 1999aa-like objects may be (photometrically) normal objects caught at very early phases. In other words, there may be two classes of SNe Ia that are photometrically normal, but spectroscopically distinct at very early times: those like SN 1999aa, which showed Fe III lines, Ca II H&K lines and no Si II 6150 Å line; and those like SN 1994D (e.g., Patat et al. 1996; Filippenko 1997) and SN 1990N (Leibundgut et al. 1991), which showed a strong Si II 6150 Å line and looked normal. If the SN 1999aa-like objects (including uncertain objects such as SN 1997cw and SN 1999gp) are counted as normal SNe Ia, the peculiarity rate in the LOSS and BAOSS sample becomes only $18\pm 4\%$ instead of $36\pm 9\%$, in agreement with the rate reported by BFN (less than 17%).

(2) The cutoff of the age bias could be as early as 1 day before peak brightness if the SN 1999aa-like objects indeed belong to the class of SN 1991T-like objects. If this is true, the simulations in Paper I indicate that LOSS and BAOSS should still discover all the SNe Ia early enough and yield the intrinsic peculiarity rate and luminosity function (Figure 15 in Paper I). Inspection of Table 1, however, shows that this may not be the case. 21 out of the 45 SNe Ia in our sample were classified later than one day before maximum, so the age bias would be significant if the cutoff were one day before maximum and our rate of SN 1991T-like objects would be only a lower limit. There are two possible reasons for this discrepancy between the observations and the simulations: (i) the age estimates

in Table 1 are quite uncertain, especially those with “0:” which were reported in the IAU Circulars as “near maximum”; and (ii) the gap between the time of discovery and the time of spectroscopic classification is simulated as a random number between 2 and 5 days in Paper I, whereas in real observations, the gap could be much larger. For example, 6 out of the 45 SNe Ia in Table 1 were spectroscopically classified more than 10 days after their discovery; the observations will therefore have a more serious age bias than the simulations done in Paper I.

An earlier cutoff for the age bias also has a direct impact on explaining the null discovery of SN 1991T-like objects in the Calán/Tololo SN survey and the SN surveys done at high redshifts (see discussions below).

The third concern is that the LOSS and BAOSS sample may suffer from uncertainties caused by small-number statistics – there are only 45 SNe Ia. While this is not a much smaller sample than the 84 SNe Ia considered by BFN, a more accurate peculiarity rate and a more precise luminosity function for SNe Ia will be obtained when more SNe are discovered by the two surveys.

The high intrinsic rate of SN 1986G/1991bg-like and SN 1991T/1999aa-like objects also suggests that they are not uncommon among observed SNe Ia, and raises the question of whether it is appropriate to categorize them as “peculiar SNe Ia.” We call them “peculiar” for historical reasons – they were rare until the past two years, and they show distinct features in their spectra. Moreover, in comparing our results with those of BFN, it is appropriate to adopt the same terminology. With such a high peculiarity rate, however, these events become an important part of the whole SN Ia sample, and they may be part of a spectroscopic/photometric sequence of SNe Ia. For example, the SN 1999aa-like objects may be the “missing link” between SN 1991T-like objects and normal events. More spectroscopic and photometric observations are needed to test these suggestions.

4.2. Comparison with the BFN Results

An advantage of the LOSS and BAOSS sample is that the SNe Ia came from well-defined SN surveys, which enables the observational biases to be well studied. In addition, the assumed extinction of SN 1991T-like objects and the adopted cutoff of the age bias, which are at present poorly constrained by observations, play negligible roles in determining the observed peculiarity rate (Paper I) – for example, all SNe are discovered regardless of the extinction used for SN 1991T-like objects (within reasonable limits). Even if SN 1991T-like objects had the apparent brightness of SN 1991bg-like objects (which means an extra R -band extinction of $A=1.4$ mag), all of them would still be discovered in the LOSS and BAOSS surveys (just as all SN 1991bg-like objects are discovered).

The situation for the SN sample used by BFN, however, is very different. The SNe

were discovered by many different groups using various survey methods. A large fraction of the SNe were discovered before 1985 when there were no systematic distance-limited SN surveys and few opportunities for rapid spectral classification. Most of the SNe in the BFN sample were discovered after maximum brightness and the spectra used to classify them were obtained even later. It is thus very difficult to disentangle the various observational biases in the sample, many of which were indeed mentioned by BFN. Moreover, since many of BFN’s SNe came from magnitude-limited surveys, the uncertain extinction of SN 1991T-like objects makes it difficult to derive the intrinsic peculiarity rate from the observed one. The observed peculiarity rate as derived by BFN (less than 17%) is thus a very rough estimate of the intrinsic one. The relatively small number for the peculiarity rate quoted by BFN can be understood primarily in the following way: (1) the sample underestimates the rate of SN 1991bg-like objects because of the light-curve shape bias and the Malmquist bias; and (2) the sample underestimates the rate of SN 1991T-like objects because of the age bias. These two reasons also probably explain why SN 1991T-like and SN 1991bg-like objects were not recognized before 1990.

4.3. Comparison with the High-Redshift Results

During the past few years, two groups have presented strong evidence that the expansion of the Universe is accelerating rather than decelerating (Riess et al. 1998; Perlmutter et al. 1999). This surprising result comes from distance measurements to about fifty SNe Ia in the redshift range $z = 0.1$ to 1, and is based on the assumption that there are no significant differences between the SNe Ia at high redshift and their low-redshift counterparts. Although this assumption is supported to first order by comparisons of the photometric and spectroscopic properties of SNe Ia at high and low redshifts (e.g., Riess et al. 1998, 2000; Coil et al. 2000), there is also some evidence for differences between SNe Ia at different redshifts. In particular, Riess et al. (1999c) tentatively point out that the risetime (from explosion to maximum brightness) of low-redshift SNe Ia as determined by Riess et al. (1999b) differs from that of their high-redshift counterparts as determined by Groom (1998) and Goldhaber (1998), although a new measurement of the high-redshift risetime by Aldering, Knop, & Nugent (2000) diminishes the significance of this difference. Also, we note that Howell, Wang, & Wheeler (2000) point out a difference in the low-redshift and high-redshift radial distributions of SNe Ia in their host galaxies. There may additionally be systematic differences in the colors of low-redshift and high-redshift SNe Ia (Falco et al. 1999).

The peculiarity rate of SNe Ia at different redshifts, if taken at face value, may be another preliminary indication that the high-redshift SNe Ia differ to some extent from their low-redshift counterparts. Our study shows that the peculiarity rate for the nearby SNe Ia is $\sim 36\%$. For the high-redshift SNe Ia, however, there has not been a single peculiar SN Ia reported among the ~ 50 spectroscopically classified SNe (Riess et al. 1998; Perlmutter

et al. 1999; Adam Riess 1999, private communication; Peter Nugent 1999, private communication). The high-redshift SN searches are magnitude-limited surveys conducted in approximately the rest-frame B band with a baseline of ~ 20 days in the rest frame. With the intrinsic luminosity function for SNe Ia derived in Section 3, the rates of SN 1991bg-like and SN 1991T-like objects can be correctly derived for the magnitude-limited surveys using the Monte Carlo simulations in Paper I. The results are shown in Figure 6 for six cases, with SN 1991T having different amounts of adopted extra extinction in the B band and two cutoffs (7 days after and 1 day before peak brightness) for the age bias. We see that the rate for SN 1991bg-like objects is less than 2%, regardless of the adopted extra extinction for SN 1991T-like objects and the cutoff of the age bias, so it is not a surprise that there have been few or no such objects discovered at high redshifts. However, if a cutoff of +7 days is used to simulate the age bias (the left panels in Figure 6), the rate for SN 1991T-like objects should be 27.3%, 18.6%, and 12.0% for the cases when SN 1991T-like objects have no extra extinction, 0.4 mag of extra extinction, and 0.8 mag of extra extinction, which means that there should be about 14 ± 3 , 9 ± 3 , and 6 ± 2 SN 1991T-like objects among the 50 high-redshift SNe Ia, respectively. The fact that there may be no clear SN 1991T-like objects in the high-redshift sample is thus surprising. A natural explanation is that there may be evolution in the characteristics of SN Ia explosions at different redshifts. The disappearance of SN 1991T-like objects at high redshift may result from the loss of certain progenitor channels at high redshift due to a possibly redshift-dependent variation in the mass, composition, and metallicity of SN Ia progenitors (e.g., Ruiz-Lapuente & Canal 1998; Livio 2000).

On the other hand, there are several other possible explanations for the null discovery of SN 1991T-like objects at high redshift. These include the following.

(1) The SNe Ia at high redshifts are very faint, and spectroscopy of them is challenging even with the world’s largest optical telescopes. Given the fact that it is often not possible even to classify SNe at high redshift, it is far more difficult to detect peculiarities in their spectra. This problem is exacerbated by the inability to view the region around redshifted Si II 6150 Å in most of the objects; it is at wavelengths inaccessible to optical spectrgraphs, and the near-infrared sky is bright. This leaves mainly the Ca II H&K lines as discriminants of peculiarity, and makes it difficult to rule out SN 1999aa-like objects (which, recall, we include here in the SN 1991T subclass). Since most of the spectra of high-redshift SNe Ia have not yet been published, we cannot assess whether the absence of reported peculiarity is significant.

(2) The SN 1991T-like objects may be extinguished by more than the maximum extinction of $A=0.8$ mag displayed in Figure 6. This higher extinction can easily make the apparent difference in the peculiarity rate at low and high redshifts statistically insignificant. To investigate this possibility we have repeated the Monte Carlo simulations in Paper I for a wide range of assumed extinctions for the SN 1991T-like objects, and the results are shown in Figure 7. As expected, the observed rate of SN 1991T-like objects drops

dramatically with an increasing adopted extinction. However, to make the null discovery of SN 1991T-like objects among the 50 high-redshift SNe Ia (assuming all have good spectra) be within the 3σ , 2σ , and 1σ confidence levels of the nearby rate, extinctions of $A=0.9$, 1.4, and 2.1 mag must be adopted for the SN 1991T-like objects. Although four known SN 1991T-like objects showed a significant amount of reddening $E(B - V)$ [SN 1991T has 0.13 mag (Filippenko et al. 1992a), SN 1995ac has 0.17 mag (Riess et al. 1999a), SN 1995bd has 0.5 mag (Riess et al. 1999a), and SN 1997br has 0.35 mag (Li et al. 1999)], the intrinsic reddening due to the SN environment is only $E(B - V) = 0.11$ mag for SN 1991T, 0.13 for SN 1995ac, 0.00 for SN 1995bd, and 0.24 for SN 1997br, when the Galactic component of the extinction is subtracted according to the map of Schlegel, Finkbeiner, & Davis (1998). Thus, the average intrinsic reddening for the four known SN 1991T-like objects is only $E(B - V) = 0.12$ mag. Assuming a normal extinction curve, the extinction in the B band would be about 0.5 mag. The requisite large extinction ($A \geq 1.1$ mag) to account for the difference between the observed rate of SN 1991T-like objects at different redshifts therefore might not be plausible.

(3) There may be a more serious age bias – that is, a cutoff earlier than +7 days for the age bias. In the discussions of Figure 5 we pointed out that the cutoff for the age bias could be as early as 1 day before peak brightness. The results for such an early cutoff are shown in the right panels of Figure 6. For a baseline of 20 days, the rate of SN 1991T-like objects is only 10%, 6%, and 4% for the case when SN 1991T-like objects have 0, 0.4 mag, and 0.8 mag of extra extinction, which means that there should be about 5 ± 2 , 3 ± 2 , and 2 ± 1 SN 1991T-like objects among the 50 high-redshift SNe Ia, respectively. The results with an early cutoff for the age bias indicate that the null discovery of SN 1991T-like objects in the high-redshift SN Ia sample is not significantly different from the cases when SN 1991T-like objects have extra extinction ($A=0.4$ or 0.8 mag).

The results from the Calán/Tololo SN Survey (CTSS) provide another compelling reason to believe that the difference between the peculiarity rate of SNe Ia at high and low redshifts is caused by the above three reasons rather than by the evolution of SNe Ia at different redshifts. The SNe Ia discovered in CTSS have redshifts of about 0.05, which is intermediate to those found at high redshift ($z \approx 0.5$) and those found by LOSS and BAOSS ($z < 0.03$). If the difference in the peculiarity rate of SNe Ia at high and low redshifts were caused by the evolution of SNe Ia, we would expect the rate of SN 1991T-like objects in CTSS to be in between these two rates. But the fact is that there are *no* apparent SN 1991T-like objects among the 31 SNe Ia discovered in the course of CTSS. CTSS and the high-redshift SN surveys have very similar characteristics: all of them are magnitude limited with a baseline of about 20 days, and all of them are done in the rest-frame B band. The null discovery of SN 1991T-like objects in these surveys at different redshifts strongly implicates the survey characteristics rather than the evolution of SNe Ia.

There is also evidence from the CTSS data that indicates serious observational biases and further supports this explanation. Mark Phillips (2000, private communication) reports

that only 23% of the SNe Ia discovered in CTSS have spectra at maximum or earlier, indicating the existence of a serious age bias. In contrast, 78% of the SNe in Table 1 were observed spectroscopically at or before maximum. Just on the basis of these numbers, one might expect that 2 of every 3 SN 1991T-like events would be classified as normal in CTSS. Hence, for the 31 SNe discovered, only 1.8 ± 1 SN 1991T-like objects would have been expected if the intrinsic rate of SN 1991T-like events were 20%. This small number is not significantly inconsistent with the fact that none of these events were found.

4.4. The Progenitor Systems of SNe Ia

As discussed in Section 1, the exact nature of the progenitor systems of SNe Ia is still unknown. Until this problem is solved, one cannot be fully confident in the use of SNe Ia for cosmological distance determinations. The favored models (for reviews see Branch et al. 1995, and Livio 2000) include the double-degenerate models which involve the coalescence of C-O white dwarf pairs, and the single-degenerate models which involve a single white dwarf accreting material from a subgiant or giant companion (systems like supersoft X-ray sources, and symbiotics).

So far the homogeneity of SNe Ia has provided a very strong restriction to the models. Because it was thought that nearly 90% of all SNe Ia form a homogeneous class in terms of their spectra, light curves, and luminosities (the BFN results), researchers have been working hard to choose a single model over all others. It has been proposed that SNe Ia in late-type and early-type galaxies may have different progenitors (e.g., Della Valle & Livio 1994; Ruiz-Lapuente, Burkert, & Canal 1995), but the homogeneity constraints of SNe Ia have served as an argument against this.

The high peculiarity rate found in our study suggests that homogeneity is no longer such a strong constraint for the progenitor systems of SNe Ia. The high peculiarity rate actually may favor the existence of different progenitor systems; with more than one class of progenitor system, SNe Ia are more likely to have different types of photometric and spectroscopic properties. For example, perhaps SN 1991bg-like objects come from double-degenerate progenitor systems, while SN 1991T-like objects have single-degenerate progenitors, or vice versa. A full discussion, however, is beyond the scope of this paper.

5. Conclusions

We have compiled a set of 45 SNe Ia discovered in the LOSS and BAOSS galaxy samples (up through SN 2000A). We find that the total observed peculiarity rate is $36 \pm 9\%$; the rates are $16 \pm 7\%$ and $20 \pm 7\%$ for SN 1991bg-like and SN 1991T-like objects, respectively. Only $64 \pm 12\%$ of observed SNe Ia are normal. Our peculiarity rate is substantially higher

than that reported by Branch, Fisher, & Nugent (1993).

LOSS and BAOSS are distance-limited SN surveys with a limiting distance where normal SNe Ia have a peak apparent magnitude of about 16.0 and 15.3, respectively. The limiting magnitude of the two surveys is about 19.0 and the baseline is ≤ 10 days. Monte Carlo simulations done by Li et al. (2000b) indicate that essentially all SNe Ia should have been found in the LOSS and BAOSS galaxies. This implies that the peculiarity rate in our sample is very close to the intrinsic one, within the uncertainties of small-number statistics. Moreover, the luminosity function of SNe Ia in our sample is also intrinsic.

We have discussed some other selection effects that may affect our results. In particular, we find that our galaxy samples are representative of the general population of bright galaxies, and that the SN 1999aa-like objects (which are similar in some ways to SN 1991T and are included here in the SN 1991T subclass) play an important role in determining the peculiarity rates.

The high rate of peculiar low-redshift SNe Ia is very different from the preliminary result found at high redshift, which is zero. However, it may be adequate to explain the difference in terms of insufficient observation quality at high redshift, extinction, and/or a serious age bias for SN 1991T-like objects. If so, it is not necessary to invoke the evolution of SNe Ia with redshift.

The high peculiarity rate at low redshifts also suggests that homogeneity is no longer such a strong argument against the existence of different progenitor systems for SNe Ia.

We acknowledge the referee, Mark Phillips, for his very useful comments on the manuscript. We also thank M. Hamuy, D. C. Leonard, and T. Matheson for helpful discussions. The work of A. V. F.'s group at U.C. Berkeley is supported by National Science Foundation grants AST-9417213 and AST-9987438, as well as by NASA grant AR-08006 from the Space Telescope Science Institute, which is operated by AURA, Inc., under NASA contract NAS5-26555. KAIT was made possible by generous donations from Sun Microsystems Inc., the Hewlett-Packard Company, AutoScope Corporation, Lick Observatory, the National Science Foundation, the University of California, and the Sylvia and Jim Katzman Foundation. We are also grateful to the National Science Foundation of China for their support of the Beijing Astronomical Observatory.

REFERENCES

- Aldering, G., Knop, R., & Nugent, P. 2000, *AJ*, 119, 2110
- Aldering, G., et al. 1999, *IAU Circ.* 7138
- Barbon, R., et al. 1990, *A&A*, 237, 79
- Branch, D., Fisher, A., & Nugent, P. 1993, *AJ*, 106, 2383 (BFN)
- Branch, D., & Tammann, G. A. 1992, *ARAA*, 30, 359
- Branch, D., et al. 1983, *ApJ*, 270, 123
- Branch, D., et al. 1995, *PASP*, 107, 1019
- Coil, A. L., et al. 2000, *ApJ*, submitted
- Cristiani, S., et al. 1992, *A&A*, 259, 63
- Della Valle, M., & Livio, M. 1994, *ApJ*, 423, L31
- de Vaucouleurs, G. 1991, *Third Reference Catalogue of Bright Galaxies* (Springer-Verlag, New York) (RC3)
- Falco, E., et al. 1999, *ApJ*, 523, 617
- Filippenko, A. V. 1997, *ARAA*, 35, 309
- Filippenko, A. V., Li, W. D., & Leonard, D. C., 1999, *IAU Circ.* 7108
- Filippenko, A. V., Metzger, M. R., & Small, T. A., 1999, *IAU Circ.* 7239
- Filippenko, A. V., et al. 1992a, *ApJ*, 384, L15
- Filippenko, A. V., et al. 1992b, *AJ*, 104, 1543
- Filippenko, A. V., et al. 2000, in preparation
- Goldhaber, G. 1998, *BAAS*, 30, 1325
- Groom, D. E. 1998, *BAAS*, 30, 1419
- Hamuy, M., et al. 1996, *AJ*, 112, 2398
- Harkness, R. P., & Wheeler, J. C. 1990, in *Supernovae*, ed. A. G. Petschek (New York: Springer-Verlag), 1
- Howell, D. A., Wang, L. F., & Wheeler, J. C., 2000, *ApJ*, 530, 166

- Jeffery, D. J., et al. 1992, *ApJ*, 397, 304
- Jha, S., et al. 1999, *ApJS*, 125, 73
- Kirshner, R. P., et al. 1973, *ApJ*, 185, 303
- Kirshner, R. P., Oke, J. B., Penston, M. V., & Searle, L. 1973, *ApJ*, 185, 303
- Kirshner, R. P., et al. 1993, *ApJ*, 415, 589
- Leibundgut, B., et al. 1991, *ApJ*, 371, L23
- Leibundgut, B., et al. 1992, *ApJ*, 401, L49
- Leibundgut, B., et al. 1993, *AJ*, 105, 301
- Li, W. D. 1999, *IAU Circ.* 7135
- Li, W. D., et al. 1996, *IAU Circ.* 6379
- Li, W. D., et al. 1999, *AJ*, 117, 2709
- Li, W. D., et al. 2000a, in *Cosmic Explosions*, eds. S. S. Holt and W. W. Zhang (New York: American Institute of Physics), 103
- Li, W. D., et al. 2000b, *ApJ*, submitted
- Li, W. D., et al. 2000c, in preparation
- Livio, M. 2000, in *Type Ia Supernovae: Theory and Cosmology* (Cambridge: Cambridge Univ. Press), in press
- Livio, M. 2000, *astro-ph/9903264*
- Maza, J., et al. 1994, *ApJ*, 424, L107
- Mazzali, P. A., et al. 1995, *A&A*, 297, 509
- Mazzali, P. A., et al. 1997, *MNRAS*, 284, 151
- Modjaz, M., & Li, W. D., 1999, *IAU Circ.* 7229
- Nugent, P., et al. 1995, *ApJ*, 455, L147
- Patat, F., et al. 1996, *MNRAS*, 278, 111
- Patat, F., et al. 1997, *A&A*, 317, 423
- Perlmutter, S., et al. 1997, *ApJ*, 483, 565

- Perlmutter, S., et al. 1999, ApJ, 517, 565
- Phillips, M. M., 1993, ApJ, 413, L105
- Phillips, M. M., et al. 1987, PASP, 99, 592
- Phillips, M. M., et al. 1992, AJ, 103, 1632
- Phillips, M. M., et al. 1999, AJ, 118, 1766
- Reiss, D. J., et al. 1998, AJ, 115, 26
- Riess, A. G., Press, W. H., & Kirshner, R. P. 1996, ApJ, 473, 588
- Riess, A. G., et al. 1998, AJ, 116, 1009
- Riess, A. G., et al. 1999a, AJ, 117, 707
- Riess, A. G., et al. 1999b, AJ, 118, 2675
- Riess, A. G., et al. 1999c, AJ, 118, 2668
- Riess, A. G., et al. 2000, ApJ, 536, 62
- Ruiz-Lapuente, P., et al. 1992, ApJ, 387, L33
- Ruiz-Lapuente, P., Burkert, A., & Canal, R. 1995, ApJ, 447, L69
- Ruiz-Lapuente, P., & Canal, R. 1998, ApJ, 497, L57
- Schlegel, D. J., Finkbeiner, D. P., & Davis, M. 1998, ApJ, 500, 525
- Schmidt, B. P., et al. 1998, ApJ, 507, 46
- Treffers, R. R., et al. 1997, IAU Circ. 6627
- Turatto, M., et al. 1996, MNRAS, 283, 1
- Turatto, M., et al. 1998, AJ, 116, 2431
- Wells, L. A., et al. 1994, AJ, 108, 2233

Fig. 1.— Spectra of SNe Ia prior to or near maximum brightness. Spectra of the normal SN Ia 1994D, two SN 1991T-like objects (SNe 1991T and 1999aa), and three SN 1991bg-like objects (SNe 1999da, 1997cn, and 1999dg) are shown. All spectra have been deredshifted. Notice the strong, broad Ca II H&K lines in the spectrum of SN 1999aa; they are very weak in SN 1991T.

Fig. 2.— Comparison of a spectrum of SN 1999bh with that of the normal SN Ia 1998bu and that of a SN 1991bg-like object SN 1997cn, all obtained about a month past maximum. All spectra have been deredshifted.

Fig. 3.— The number of galaxies in the LOSS galaxy sample versus the expected peak apparent magnitude of SNe Ia in the galaxies.

Fig. 4.— The ratio of the LOSS sample galaxies to the RC3 galaxies for different galaxy Hubble types. A total of 9,800 galaxies is used from RC3. The ratio has been normalized by the different number of galaxies in the two sets of galaxies. The dotted line is ratio = 1.

Fig. 5.— Spectra of SNe near maximum brightness. Spectra of three SN 1991T-like (actually 1999aa-like) objects are shown with that of the normal SN Ia 1994D.

Fig. 6.— The observed peculiarity rate for the magnitude-limited surveys in the B band. Here the intrinsic peculiarity rate of SNe Ia found in the LOSS and BAOSS is adopted. The left panels show the results for a cutoff of +7 days for the age bias, while the right panels show those for a cutoff of -1 day. Three cases with SN 1991T-like objects having different extinctions are shown for each cutoff. In each case, the rate of SN 1991bg-like objects is shown as a dashed line, the SN 1991T-like objects as a dash-dotted line, and the total peculiarity rate as a solid line. See Paper I for the details of the Monte Carlo simulations.

Fig. 7.— The observed rate of SN 1991T-like objects in magnitude-limited surveys in the B band with a baseline of 20 days and different adopted extinctions. As in Fig. 6, the intrinsic rate found in LOSS and BAOSS is adopted.

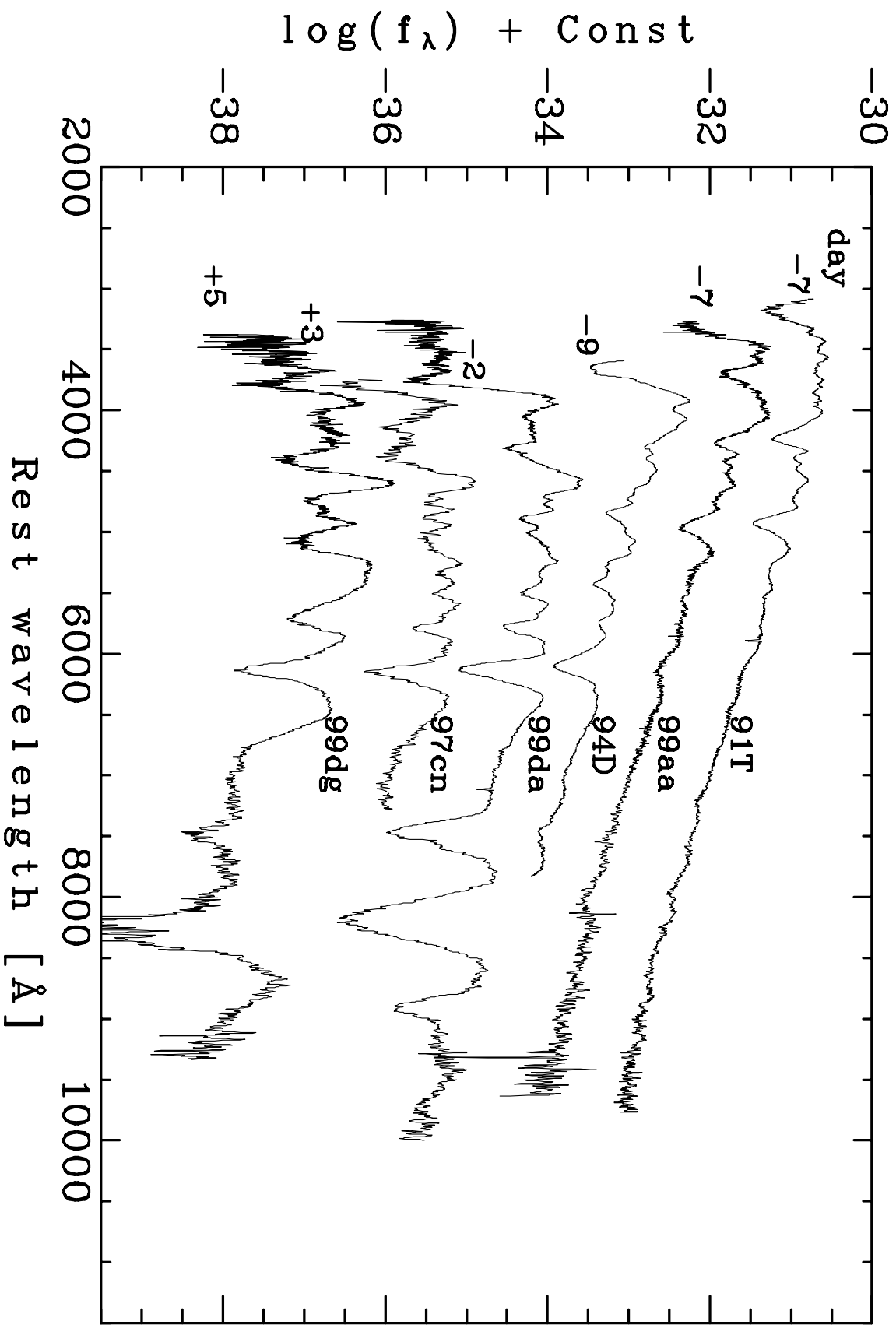


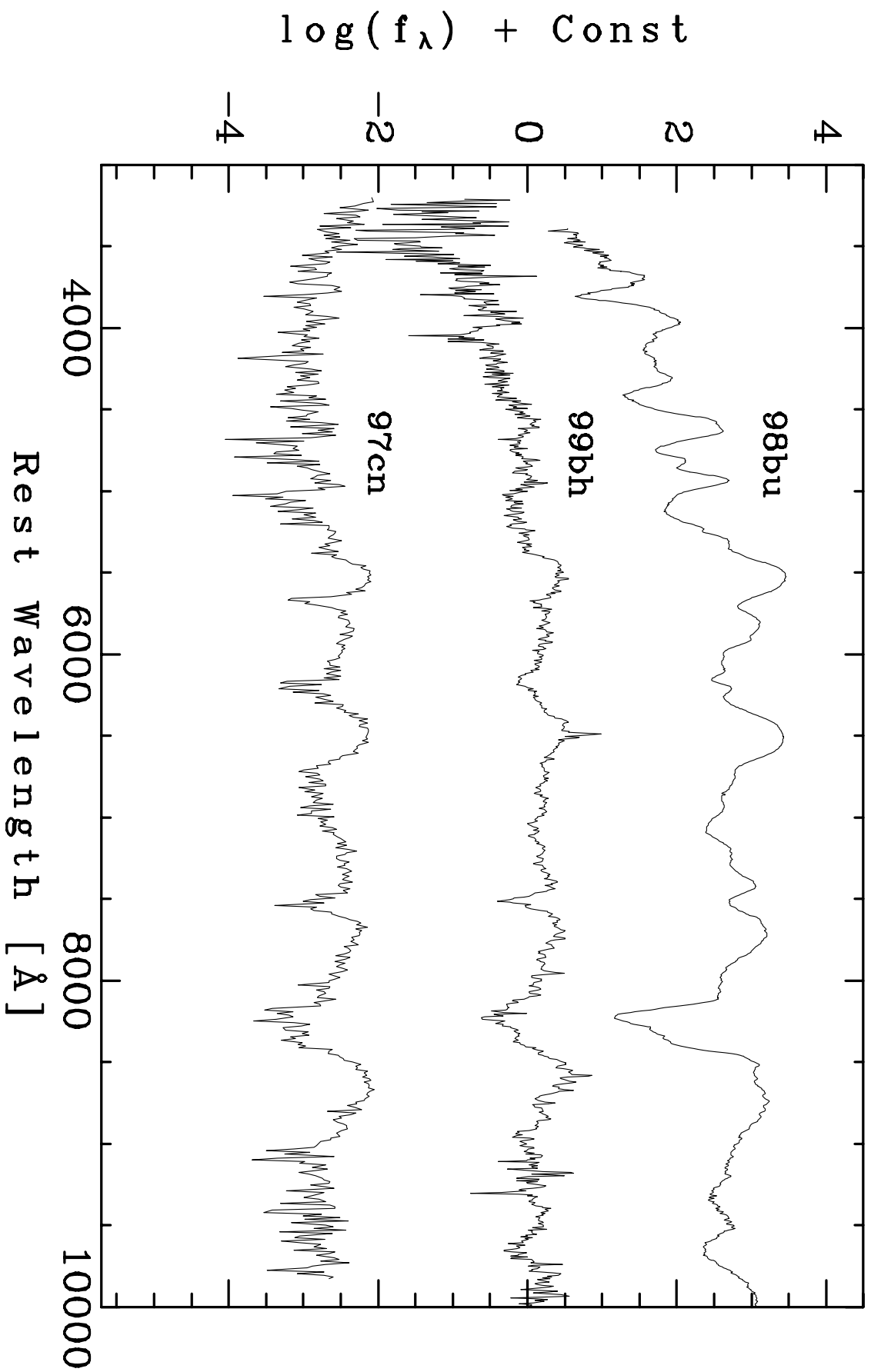
Table 1. Sample of SNe Ia

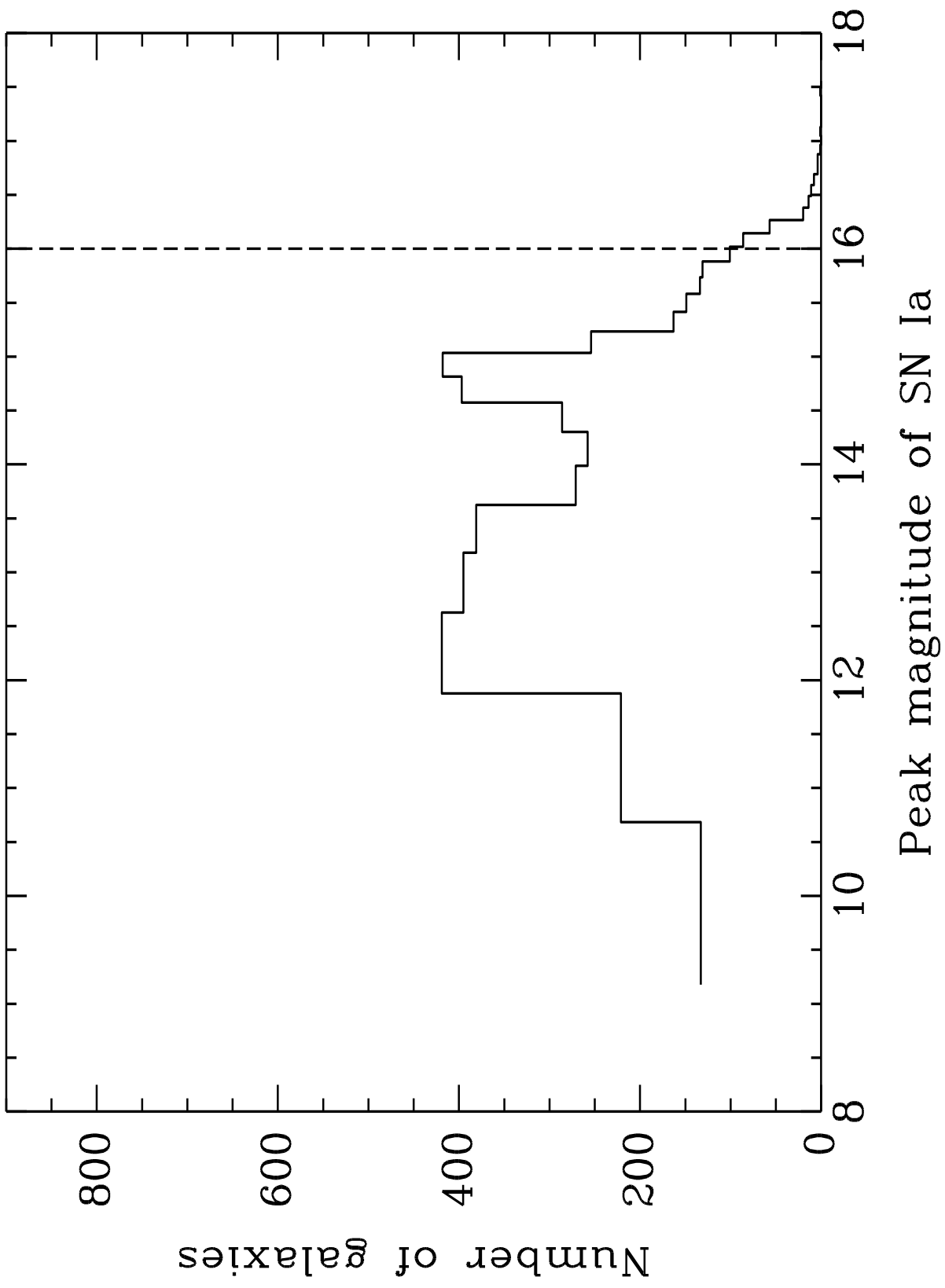
SN	Galaxy	G type	IAUC	t	T	pec?	Ti	Si5	Fe	Si6
1997Y	NGC 4675	SBb:	6557	0:	B					
1997bq	NGC 3147	Sbc	6616	−7	O					
1997br	ESO 576-G40	SBd:	6623	−9	B	91T			y	y
1997cn	NGC 5490	E	6667	1	B	91bg	y	y		
1997cw	NGC 105	Sab:	6699	0:	B	91T/91T _{aa}			y	y
1997dg	A 234014+2	S:	6749	0:	B					
1997do	UGC 3845	SBbc	6766	−7	B					
1997dt	NGC 7448	Sbc	6775	−7:	B					
1998D	NGC 5440	Sa	6815	0:	B					
1998V	NGC 6627	SBb	6844	0:	O					
1998ab	NGC 4704	SBbc	6858	−7	B	91T _{aa}			y	y
1998an	UGC 3683	S0	6878	0:	O					
1998aq	NGC 3982	Sb:	6880	−7	O					
1998bn	NGC 4462	SBab	6888	−4	L					
1998bp	NGC 6495	E	6890	0:	O	86G/91bg	y	y		
1998bu	NGC 3368	Sab	6905	−7	O					
1998de	NGC 252	S0	6980	−8	L	91bg	y	y		
1998dh	NGC 7541	SBbc	6980	−10	L					
1998dj	NGC 788	S0/a	6990	18: ^a	L					
1998dk	UGC 139	Sc:	6997	0:	L					
1998dm	MCG -01-04-4	Scd:	6997	−9	L					
1998dx	UGC 11149	Sb	7011	0:	L					
1998eb	NGC 1961	Sc	7018	25: ^a	L					
1998ec	UGC 3576	SBb	7024	−5:	L					
1998ef	UGC 646	SB:	7032	−9	L					
1998es	NGC 632	S0:	7054	−9	L	91T _{aa}			y	y
1999aa	NGC 2595	S	7108	−9	O	91T _{aa}			y	y
1999ac	NGC 6063	S	7122	−9	L	91T _{aa}			y	y
1999bh	NGC 3435	Sb	7137	7:	L	86G/91bg				
1999by	NGC 2841	Sb	7159	−14	L	91bg	y	y		
1999cl	NGC 4501	SAb	7190	−7	L					
1999cp	NGC 5468	Scd	7206	−10	L					
1999cw	MCG 01-02-0	Sab	7216	0:	L	91T _{aa}			y	y
1999da	NGC 6411	E	7218	−7	L	91bg	y	y		
1999dg	UGC 9758	S0	7239	7: ^b	L	91bg				
1999dk	UGC 1087	Sc	7238	−14	L					
1999do	MRK 922	Scd:	7252	9: ^b	L					
1999dq	NGC 976	Sc:	7250	−10	L	91T _{aa}			y	y
1999ej	NGC 495	S0/a	7298	−2 ^b	L					
1999ek	UGC 3329	Sbc	7300	+2: ^b	L					
1999gd	NGC 2623	Pec.	7328	0: ^b	L					
1999gf	UGC 5515	E	7328	+60: ^a	L					
1999gm	PGC 24106	S0	7334	0:	L					
1999gp	UGC 1993	Sb	7341	0: ^b	L	91T/91T _{aa}			y	y
2000A	MCG +1-59-81	Sa	7341	0:	L					

Note: see text for details.

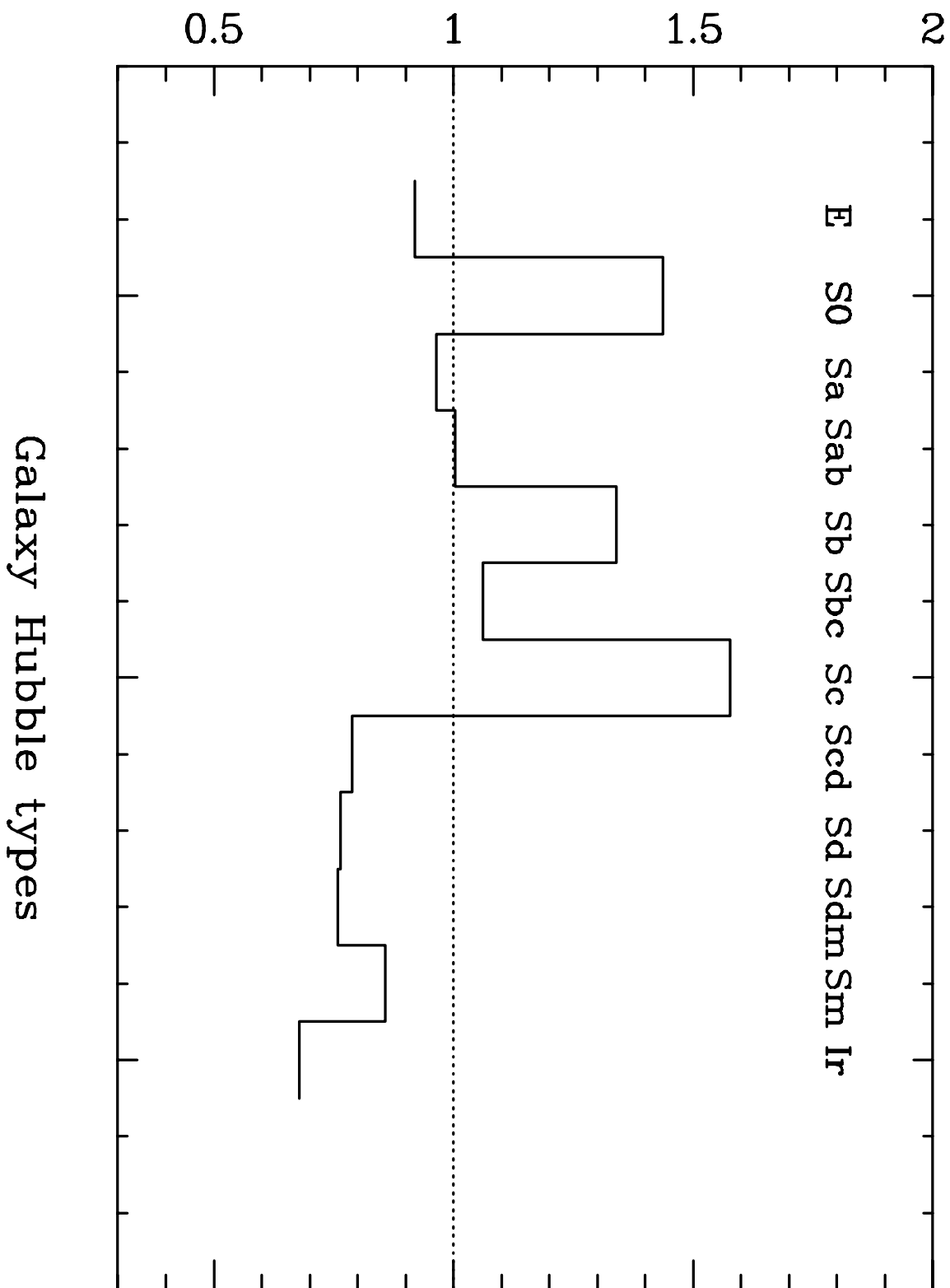
^aDiscovered in the first image after a long break.

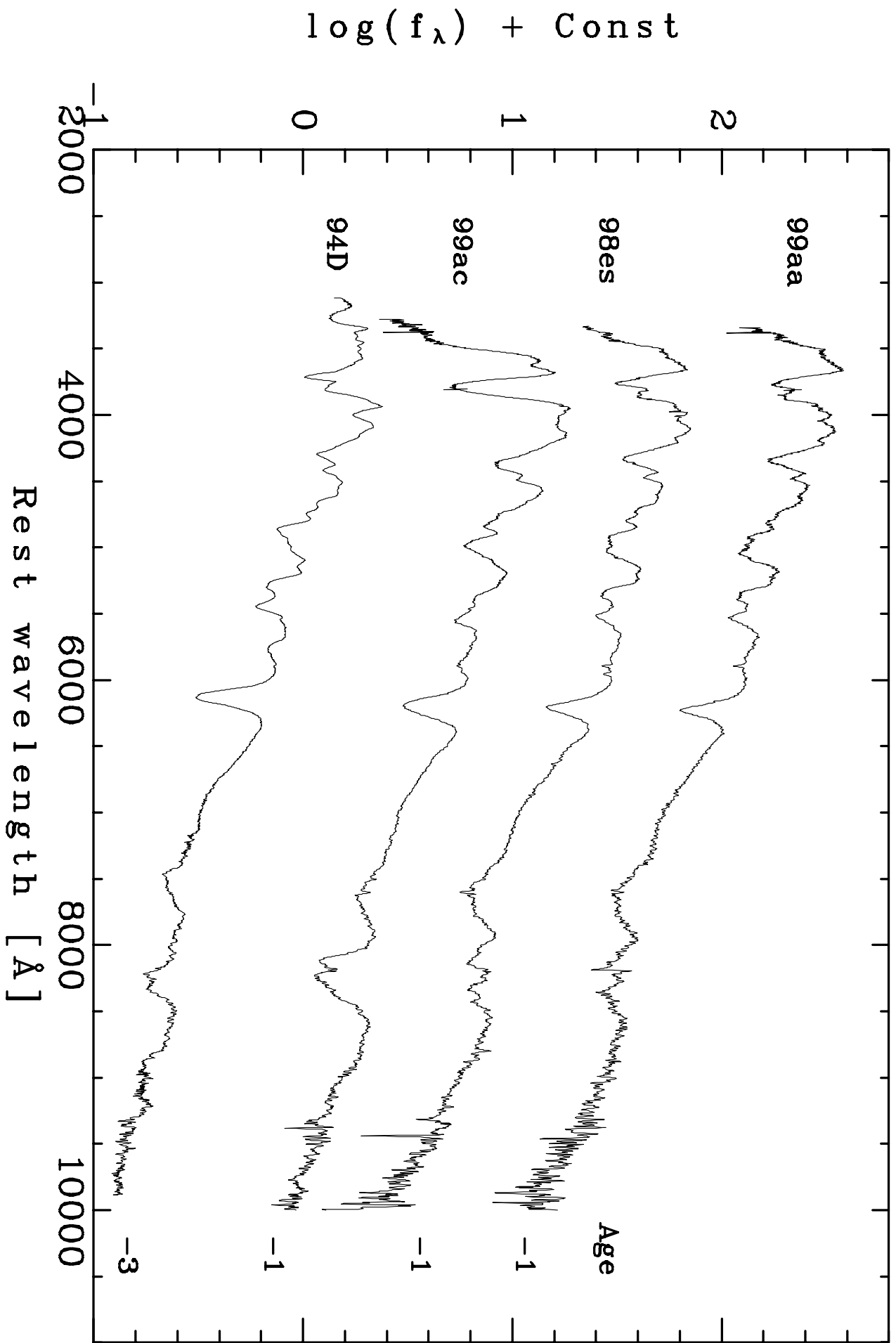
^bClassification done more than 10 days after discovery.



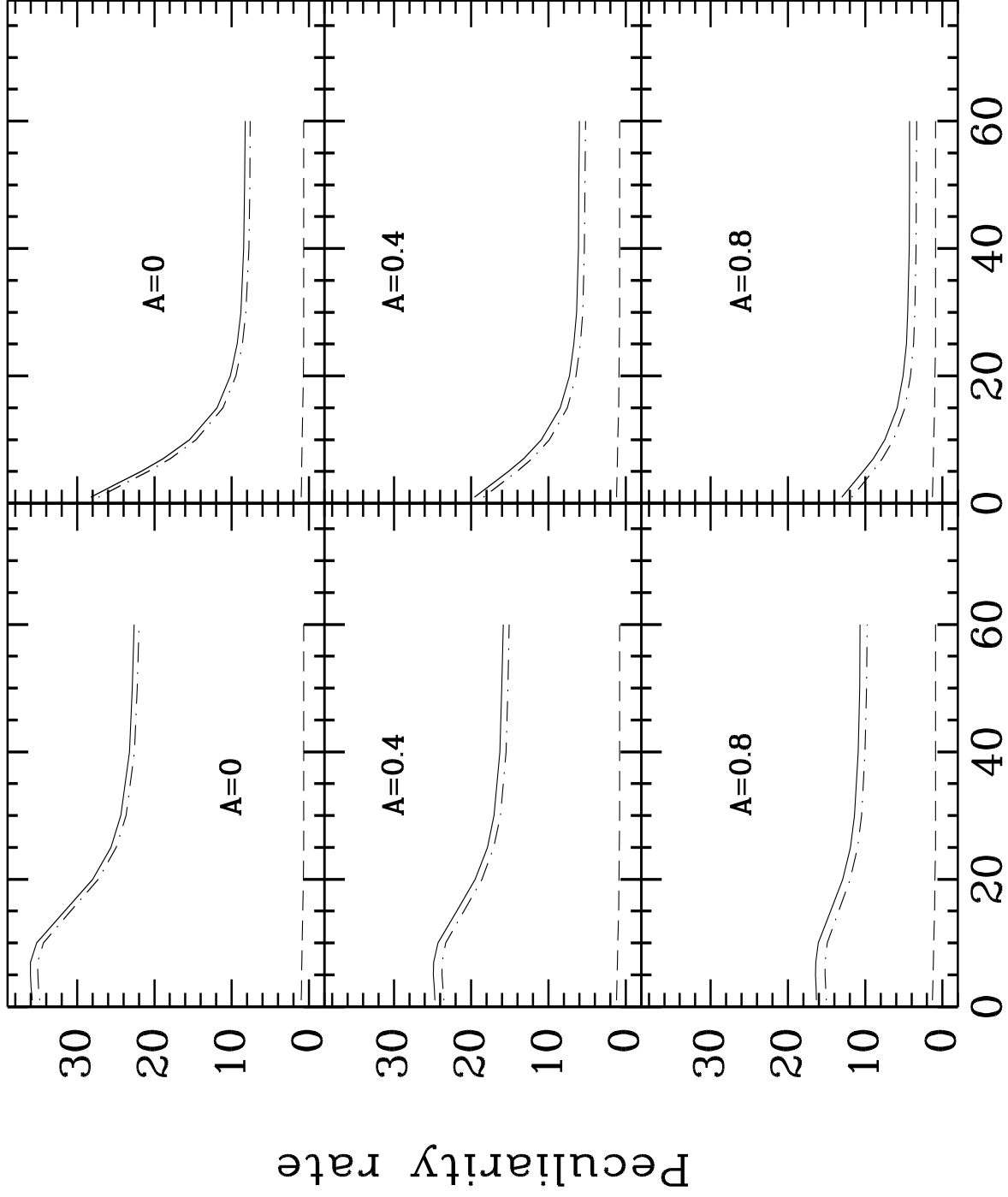


Relative ratio





Cutoff = +7 days Cutoff = -1 day



Baseline (days)

